

DEUTSCHES ELEKTRONEN-SYNCHROTRON **DESY**

DESY 75/41
October 1975

DESY-Bibliothek
14. NOV. 1975

Electroproduction of Neutral Pions in the Resonance Region

by

J.-C. Alder, F. W. Brasse, W. Fehrenbach, J. Gayler, S. P. Goel,
R. Haidan, V. Korbel, J. May, M. Merkwitz, A. Nurimba

2 HAMBURG 52 . NOTKESTIEG 1

Electroproduction of Neutral Pions in the
Resonance Region

J.-C. Alder⁺, F.W. Brasse, W. Fehrenbach⁺⁺, J. Gayler, S.P. Goel⁺⁺⁺,
R. Haidan, V. Korbel⁺⁺⁺⁺, J. May⁺⁺⁺⁺, M. Merkwitz, A. Nurimba

Deutsches Elektronen-Synchrotron DESY, Hamburg, Germany

ABSTRACT

Results on the reaction $ep \rightarrow e'p\pi^0$ are presented in the mass range $1.355 \leq W \leq 1.745$ GeV at $q^2 \approx 1$ GeV² and in the range $1.415 \leq W \leq 1.595$ GeV at $q^2 \approx 0.6$ GeV².

From the angular distribution of the π^0 meson the polarization terms $\sigma_U + \epsilon\sigma_L$, σ_P and σ_I have been determined in a range of production angles from $\theta^* \gtrsim 50^\circ$ up to $\theta^* = 180^\circ$. Results on the total $\gamma_V p \rightarrow \pi^0 p$ cross section are given.

Present addresses:

- + Université de Lausanne
- ++ Babcock-Brown-Boveri, Mannheim
- +++ On leave from Kurukshetra University, Kurukshetra, India
- ++++ CERN, Geneva

INTRODUCTION

We have reported on an experiment on electroproduction of η -mesons¹⁾ and π^+ -mesons²⁾ in the resonance region. Now we report on the data of the reaction $ep \rightarrow ep\pi^0$ taken at the same experiment.

There exist data on π^0 production from Daresbury at $q^2 \approx 0.4$ and 0.6 GeV^2 ³⁾ in the second resonance region and some data from DESY⁴⁾ in the third resonance region and above in a limited angular range. The present experiment covers the second resonance region ($q^2 \approx 0.6, 1 \text{ GeV}^2$) and the third resonance region ($q^2 \approx 1 \text{ GeV}^2$). The obtained angular distributions have been analysed in terms of the polarization terms $\sigma_U + \epsilon\sigma_L$, σ_P and σ_I .

In a recent multipole analysis of the existent data on pion production Devenish and Lyth⁵⁾ described the resonance region in terms of 11 resonances. These authors also used a preliminary subset of the present data. It is the purpose of the present experiment to allow for a determination of the couplings of the relevant resonances in the covered kinematic range.

NOTATION

We express the cross section in terms of the virtual photon absorption cross section $d\sigma/d\Omega_{\pi^0}^*$ in the CMS of the final hadrons which is related to the differential coincidence cross section $d^5\sigma/dE' d\Omega_e d\Omega_{\pi^0}^*$ by the virtual photon flux factor Γ_t (defined as usually⁶⁾):

$$\frac{d^5\sigma}{dE' d\Omega_e d\Omega_{\pi^0}^*} = \Gamma_t \frac{d\sigma}{d\Omega_{\pi^0}^*} \quad (1)$$

The polar and azimuthal production angles (fig. 1) in the CMS are denoted by θ^* and ϕ . The ϕ dependence of the angular distribution in the CMS can be written explicitly as⁷⁾:

$$\frac{d\sigma}{d\Omega_{\pi^0}^*} = \sigma_U + \epsilon\sigma_L + \epsilon \cos 2\phi \sigma_P + \sqrt{2\epsilon(\epsilon+1)} \cos\phi \sigma_I \quad (2)$$

The parameter ϵ describes the polarization of the virtual photon (e.g. ref. 6). The cross sections σ_U , σ_L , σ_P and σ_I are functions of the invariant mass W of the final $p\pi^0$ system, the momentum transfer q^2 , and the angle θ^* .

The terms σ_U and σ_L are the cross sections of unpolarized transverse and longitudinal virtual photons. They can only be separated by changing the polarization ϵ , not done in this experiment. σ_P takes account of the transverse polarization of the virtual photon and σ_I is a transverse-longitudinal interference term. A study of the ϕ dependence for fixed θ^* allows to separate the 3 terms $\sigma_U + \epsilon\sigma_L$, σ_P and σ_I .

If in addition to one photon exchange we assume that only S, P and D waves contribute, with total angular momentum $j \leq 3/2$, we can express the cross section in terms of angular coefficients (cf. e.g. ref. 3):

$$\begin{aligned} \sigma_U + \epsilon\sigma_L &= \bar{A}_0 + \bar{A}_1 \cos\theta^* + \bar{A}_2 \cos^2\theta^* + \bar{A}_3 \cos^3\theta^* \\ \sigma_P &= (C_0 + C_1 \cos\theta^*) \sin^2\theta^* \\ \sigma_I &= (D_0 + D_1 \cos\theta^* + D_2 \cos^2\theta^*) \sin\theta^* \end{aligned} \quad (3)$$

If we allow for F waves with $j = 5/2$ the following 3 terms $\bar{A}_4 \cos^4\theta^*$, $C_2 \cos^2\theta^* \sin^2\theta^*$, $D_3 \cos^3\theta^* \sin\theta^*$ have to be added. The total virtual photoproduction cross section is then given by:

$$\sigma_{\text{tot}} = 4\pi \left(\bar{A}_0 + \frac{1}{3} \bar{A}_2 + \frac{1}{5} \bar{A}_4 \right) \quad (4)$$

APPARATUS

The experimental setup is described in more detail in ref. 1. Only a short description is repeated here. The measurements are done in an external e^- beam of DESY. The primary beam hits a 12 cm liquid hydrogen target. The intensity is controlled by a secondary emission monitor, which was compared many times during the experiment to a Faraday cup. The scattered electron is detected in a double focussing vertically bending spectrometer. It is identified by a threshold Cerenkov- and a sandwich shower counter.

The secondary proton is detected in coincidence with the scattered e^- in a non focussing spectrometer consisting of a vertically bending magnet, a system of proportional chambers mounted at the magnet exit, and a scintillator hodoscope.

DATA ANALYSIS

The secondary protons are distinguished from π^+ mesons by time of flight¹⁾. Some pion background in the remaining proton sample was rejected by requirement of sufficient pulse height of scintillator signals.

The reaction $ep \rightarrow ep\pi^0$ was determined by the requirement of appropriate missing mass, computed from the detected electron and proton. An example of a missing mass squared distribution is given in fig. 2. Events in the range of missing mass squared from - 0.02 to 0.07 GeV^2 have been used to calculate the cross sections of the reaction $ep \rightarrow ep\pi^0$.

Acceptances and various corrections have been calculated by a Monte Carlo simulation of the experiment. Radiative corrections have been incorporated into the simulation including internal and external radiation. In this simulation the radiation of the electron has been taken into account in the peaking approximation according to the formulas of ref. 8). Some multipion background has also been included into the simulation, leading to corrections smaller than 3 %.

The cross sections are corrected for empty target rate ($\approx 0.5\%$), nuclear absorption ($\approx 1.5\%$), dead time losses, inefficiencies, multi track events and random background.

RESULTS

All data have been taken with the central electron spectrometer angle set to 15° . The polarization ε was always close to 0.9. The errors given in the figures are statistical only. We estimate an overall systematic error of 6 %.

The measured angular distributions range from forward to backward production angles in some cases. The polarization terms $\sigma_U + \varepsilon\sigma_L$, σ_P and σ_I have been determined by least squares fits of the differential cross sections at fixed W , q^2 and $\cos\theta^*$ according to the ϕ dependence of eq. (2). Results of these fits are given in figs. 5 to 7 and table 1 only if a range in ϕ of at least 100° is covered. This is the case essentially in the backward hemisphere. The backward cross sections $\sigma_U + \varepsilon\sigma_L$ (fig. 3) have been obtained by averaging over all events of a given W , q^2 -bin with $\cos\theta^* < -0.97$.

We estimated the total cross section σ_{tot} of $\gamma_{\nu} p \rightarrow \pi^0 p$ in some range of W , where the angular coverage was sufficient. σ_{tot} was computed according to eq. (4) from the angular coefficients which were determined by least squares fits to all differential cross sections of a given W , q^2 -bin. For $W \leq 1.565$ GeV eq. (3) has been used. For larger W values the coefficients \bar{A}_4 , C_2 and D_3 have been included. The curves in figs. 4 to 6 represent the cross sections according to these fits. The results on σ_{tot} are given in table 2 and in fig. 8 together with the results⁹⁾ of a previous experiment⁶⁾. Due to lack of acceptance there may be considerable errors at $q^2 = 0.6$ GeV² and at $W \gtrsim 1.6$ GeV at $q^2 = 1$ GeV². Total $\gamma_{\nu} p \rightarrow X$ cross sections are shown for comparison.

We have compared our results with the data of Shuttleworth et al.³⁾ and Driver et al.⁴⁾. In general we find that our differential cross sections are consistent with both experiments. A comparison with the Daresbury data³⁾ is shown in figs. 3 and 4. Our results on total cross sections at $q^2 = 0.6$ GeV² (table 2) on the other hand are systematically below those

from ref. 3) by about 25 %.

A complete list of all measured differential cross sections will be given elsewhere.

The backward cross sections (fig. 3) show considerable structure in the third resonance region indicating the presence of resonant amplitudes of total helicity 1/2 of the ingoing virtual photon and proton. In the second resonance region helicity 3/2 excitation seems to be more important than helicity 1/2 excitation: At W about 1.5 GeV the backward cross sections are very small and show no significant resonance structure (fig. 3) and the angular distributions (figs. 4,5 and 6) are similar to those observed in photoproduction. It is one of the results of the multipole analysis of Devenish and Lyth⁵⁾, that helicity 1/2 excitation increases in relative importance as q^2 changes from zero to a few GeV^2 . Moreover this increase seems to occur more rapidly at $F_{15}(1688)$ than at $D_{13}(1525)$. In this analysis⁵⁾ some preliminary differential cross sections of the present experiment with ϕ close to 90° had been used.

As shown in a recent experiment¹⁰⁾ the angular distribution of the reaction $ep \rightarrow ep\pi^0$ at $W \approx 2.55$ GeV changes rapidly going from photoproduction to space-like four momentum transfers. It was remarked by Moorhouse¹¹⁾ that this change may be foreshadowed in the region of $F_{15}(1688)$ just as the dip at $t \approx -0.5 \text{ GeV}^2$ and the subsequent hump first appears in this region in photoproduction. The present data cover the range from $t \approx -0.5 \text{ GeV}^2$ up to the backward direction at $W \gtrsim 1.688$ GeV. It is interesting to note that the cross section at $q^2 = 1 \text{ GeV}^2$ (fig. 4) essentially decreases from $t = -0.5 \text{ GeV}^2$ ($\cos\theta^* \approx 0.65$) to $t = -1.4 \text{ GeV}^2$ ($\cos\theta^* \approx -0.15$) or even up to $t \approx -2 \text{ GeV}^2$ ($\cos\theta^* \approx -0.65$) without the strong rise observed at $q^2 = 0$ at $|t| \gtrsim 0.5 \text{ GeV}^2$.

Acknowledgements

We gratefully acknowledge the excellent performance of the Synchrotron crew, the Hallendienst and the Rechenzentrum. We thank J. Koll, G. Singer, K. Thiele, H. Weiß and Mrs. K. Schmöger for careful technical work, E. Ganßauge for his help in the early stage of the experiment.

References

1. J.-C. Alder, F.W. Brasse, W. Fehrenbach, J. Gayler, R. Haidan, G. Glöe, S.P. Goel, V. Korbel, W. Krechlok, J. May, M. Merkwitz, R. Schmitz, W. Wagner, Nucl. Phys. B91 (1975)386
2. J.-C. Alder et al., DESY 75/29 (1975), Nucl. Phys. B
3. W.J. Shuttleworth, A. Sofair, R. Siddle, B. Dickinson, M. Ibbotson, R. Lawson, H.E. Montgomery, R.D. Hellings, J. Allison, A.B. Clegg, F. Foster, G. Hughes, P.S. Kummer, Nucl. Phys. B45 (1972)428
4. C. Driver, K. Heinloth, K. Höhne, G. Hofmann, P. Karow, D. Schmidt, G. Specht, J. Rathje, Nucl. Phys. B33 (1971)84
5. R.C.E. Devenish, D.H. Lyth, Nucl. Phys. B93 (1975)109
6. e.g. J.-C. Alder et al., Nucl. Phys. B46 (1972)573
7. K. Berkelman, Proceedings of the Int. Symposium on Electron and Photon Interactions at High Energies, Hamburg, 1965
M. Gourdin, Nuovo Cimento 21 (1961)1094
8. G. Miller, Thesis, Stanford University (1971)
9. J. Gayler, Thesis, DESY F21-71/2 (1971)
J. May, Thesis, DESY F21-71/3 (1971)
10. F.W. Brasse, W. Fehrenbach, W. Flauger, J. Gayler, S.P. Goel, R. Haidan, U. Kötz, V. Korbel, D. Kreinick, J. Ludwig, J. May, M. Merkwitz, K.-H. Mess, P. Schmüser, B.H. Wiik, DESY 75/23 (1975)
11. R.G. Moorhouse, Rapporteur's talk presented at the Palermo Conference, June 1975
12. F.W. Brasse, W. Flauger, J. Gayler, S.P. Goel, R. Haidan, M. Merkwitz, H. Wriedt, DESY 75/ (1975)

$\cos\theta^*$	$\sigma_{U+\epsilon\sigma_L}$	σ_P	σ_I	$\cos\theta^*$	$\sigma_{U+\epsilon\sigma_L}$	σ_P	σ_I
	(ub / sr)				(ub / sr)		
-0.985	0.88 ± 0.11	-0.20 ± 0.13	-0.02 ± 0.06	-0.985	0.41 ± 0.03	-0.10 ± 0.05	0.02 ± 0.02
-0.950	1.16 ± 0.20	-0.40 ± 0.16	-0.06 ± 0.07	-0.950	0.56 ± 0.05	-0.05 ± 0.08	-0.03 ± 0.05
-0.900	1.35 ± 0.09	-0.70 ± 0.19	-0.21 ± 0.08	-0.900	0.73 ± 0.03	-0.32 ± 0.05	-0.01 ± 0.02
-0.850	1.73 ± 0.11	-0.90 ± 0.22	-0.09 ± 0.09	-0.850	0.82 ± 0.04	-0.14 ± 0.08	-0.05 ± 0.04
-0.800	1.88 ± 0.12	-0.90 ± 0.30	0.03 ± 0.13	-0.800	0.85 ± 0.04	-0.03 ± 0.05	-0.05 ± 0.03
-0.750	2.13 ± 0.15	-0.31 ± 0.41	-0.21 ± 0.17	-0.750	0.88 ± 0.04	-0.03 ± 0.06	-0.03 ± 0.04
-0.700	2.62 ± 0.21	-0.13 ± 0.57	-0.08 ± 0.22	-0.700	0.94 ± 0.04	-0.03 ± 0.10	-0.04 ± 0.05
-0.650	2.67 ± 0.28	-0.84 ± 0.38	-0.06 ± 0.16	-0.650	1.10 ± 0.11	-0.27 ± 0.15	-0.09 ± 0.12
-0.600	2.50 ± 0.21	-0.90 ± 0.33	-0.03 ± 0.15	-0.600	0.85 ± 0.19	-0.46 ± 0.22	0.06 ± 0.16
-0.550	2.25 ± 0.17	-1.18 ± 0.34	-0.04 ± 0.18				
-0.500	2.60 ± 0.19	-1.28 ± 0.33	-0.15 ± 0.18				
-0.450	2.48 ± 0.21	-0.95 ± 0.37	-0.11 ± 0.19				
-0.400	1.93 ± 0.18	-1.28 ± 0.33	-0.15 ± 0.18				
-0.350	1.63 ± 0.20	-1.10 ± 0.31	-0.23 ± 0.19				
-0.300	1.58 ± 0.29	-0.18 ± 0.35	-0.22 ± 0.25				
-0.250							
-0.200							
-0.150							
-0.100							
0.050							
0.100							
0.150							
0.200							
0.250							
0.300							
0.350							
0.400							
0.450							
0.500							
0.550							
0.600							
0.650							
0.700							
0.750							
0.800							
0.850							
0.900							
0.950							
0.985							

Table 1. Angular distributions of the reaction $\gamma_{\text{D}} \rightarrow \pi^0 p$. The errors do not contain an overall systematic error of 6 %.

Table 2: Estimates of σ_{tot} of $\gamma_{\nu} p \rightarrow \pi^0 p$ from the fitted angular coefficients (see text).
The errors are statistical only.

W [GeV]	σ_{tot} [μb] $q^2 \approx 1 \text{ GeV}^2$	σ_{tot} [μb] $q^2 \approx 0.6 \text{ GeV}^2$
1.325	30.9 ± 2.7	
1.355	22.2 ± 0.6	
1.385	16.4 ± 0.4	
1.415	14.2 ± 0.4	22.5 ± 4.1
1.445	14.3 ± 0.4	21.0 ± 2.9
1.475	15.8 ± 0.6	18.2 ± 4.3
1.505	18.4 ± 1.0	16.4 ± 4.9
1.535	18.2 ± 1.5	18.6 ± 7.0
1.565	13.2 ± 1.5	
1.595	15.0 ± 3.4	
1.625	16.6 ± 4.1	
1.655	10.5 ± 5.1	
1.685	10.1 ± 6.6	
1.715	13.9 ± 7.4	

Figure Captions

- Fig. 1: Definition of the angles.
- Fig. 2: Example of a distribution of missing mass squared computed from the detected protons in coincidence with electrons.
- Fig. 3: Backward π^0 production cross sections as a function of W at $q^2 = 0.6 \text{ GeV}^2$ from DNPL³⁾ and at $q^2 = 0.6$ and 1 GeV^2 from this experiment.
- Fig. 4: Examples of angular distributions at $q^2 = 0.6 \text{ GeV}^2$ in comparison with data from DNPL³⁾ and at $q^2 = 1 \text{ GeV}^2$ from this experiment. Solid line: cross section computed from the angular coefficients (see text).
- Fig. 5: Angular distribution of $\sigma_U + \epsilon\sigma_L$ (∇), σ_P (\square) and σ_I (\circ) at $q^2 = 0.6 \text{ GeV}^2$. Curves: $\sigma_U + \epsilon\sigma_L$ (-), σ_P (--), and σ_I (***). as computed from the angular coefficients (see text).
- Fig. 6: a) Angular distributions of $\sigma_U + \epsilon\sigma_L$ (∇), σ_P (\square), and σ_I (\circ) at $q^2 = 1 \text{ GeV}^2$ in the W range 1.355 GeV to 1.565 GeV . Curves: $\sigma_U + \epsilon\sigma_L$ (-), σ_P (--), and σ_I (***). as computed from the angular coefficients (see text).
b) Same as fig. 6a) in the W range 1.595 GeV to 1.745 GeV .
- Fig. 7: $\sigma_U + \epsilon\sigma_L$ (∇), σ_P (\square) and σ_I (\circ) as a function of W at different values of $\cos\theta^*$ at $q^2 = 1 \text{ GeV}^2$.
- Fig. 8: Total cross section of $\gamma_{\nu}p \rightarrow \pi^0 p$ (∇ from ref 9, \blacktriangledown this experiment) in comparison to the total cross section of $\gamma_{\nu}p \rightarrow X$ (\circ from ref. 12).

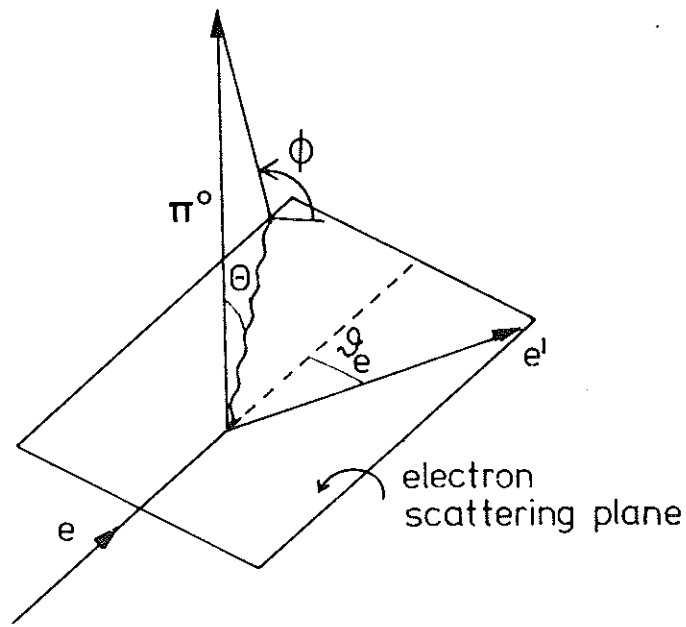


Fig. 1

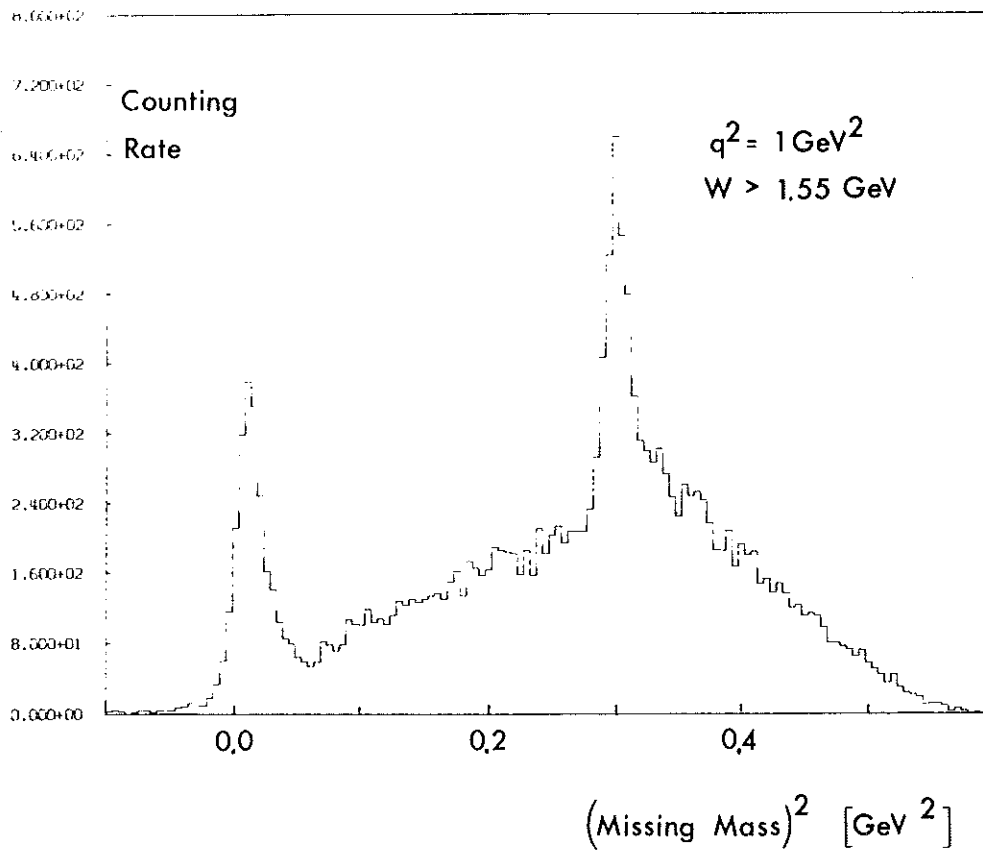
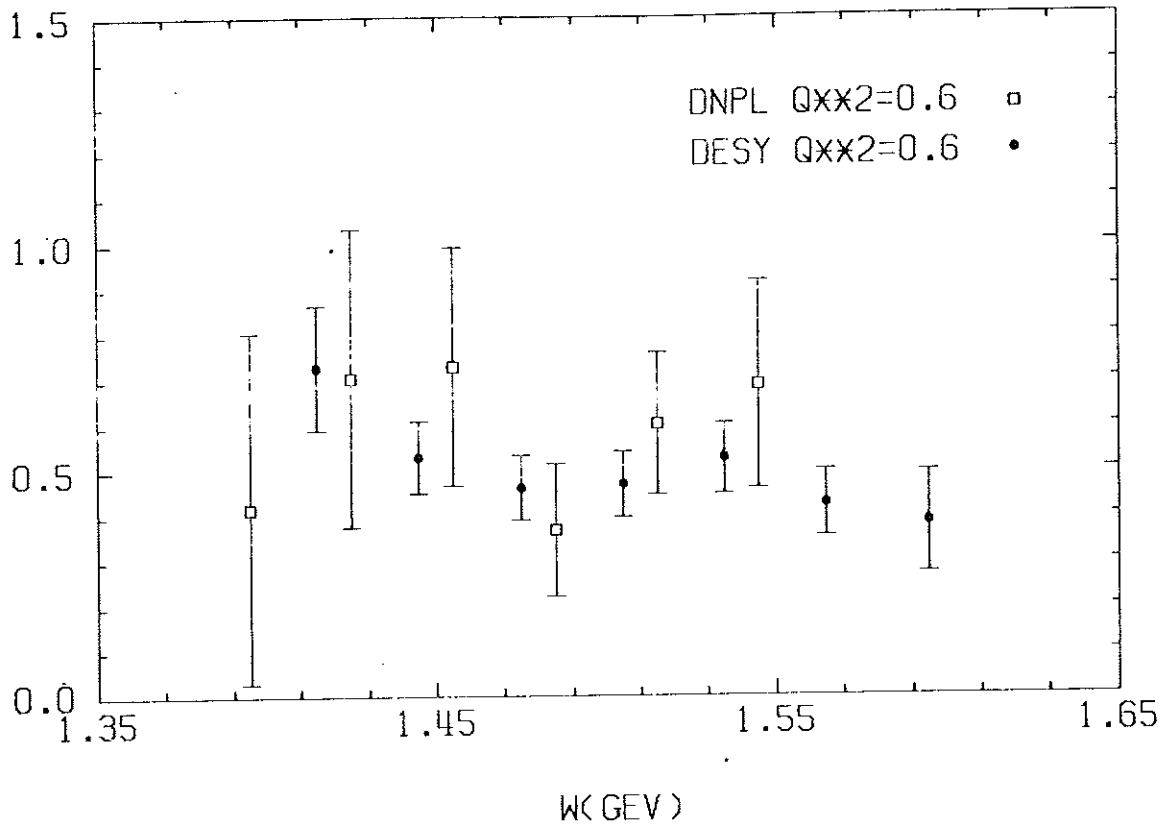


Fig. 2

$$\gamma_{\nu} p \rightarrow \pi^0 p,$$

$$\theta_{\pi^0}^* \approx 180^\circ$$

$$\frac{d\sigma}{d\Omega^*} (\mu\text{b/sr})$$



$$\frac{d\sigma}{d\Omega^*} (\mu\text{b/sr})$$

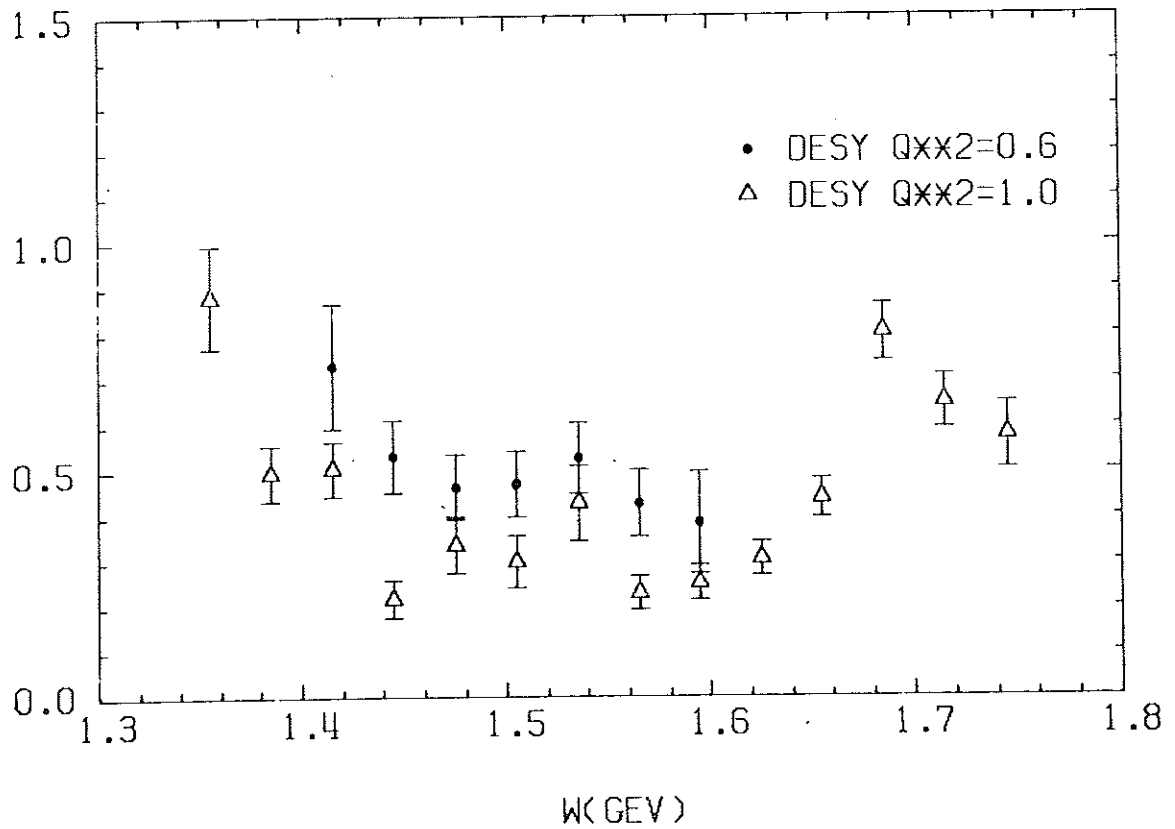


Fig. 3

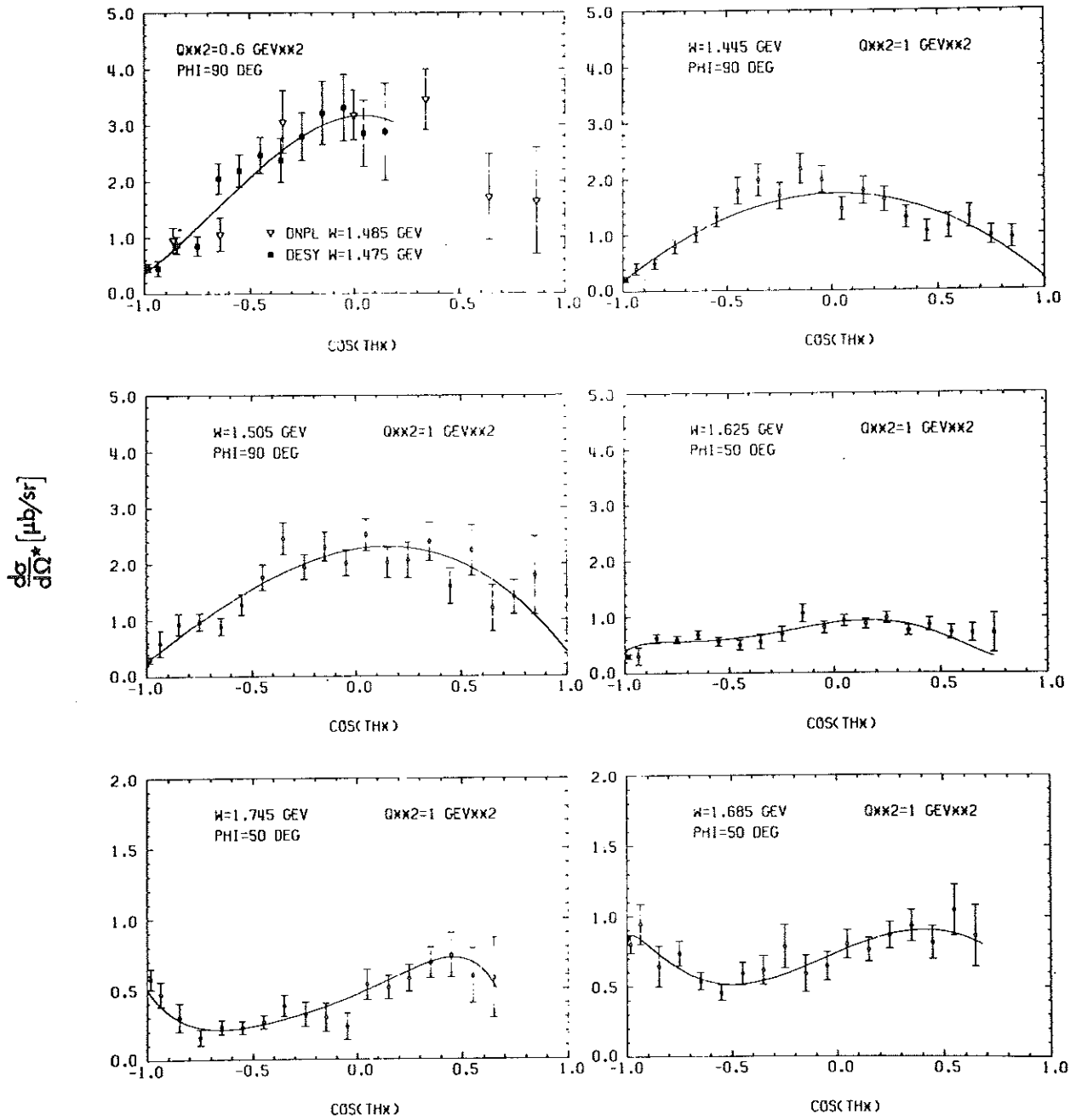
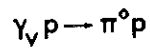


Fig. 4

$\gamma p \rightarrow \pi^0 p$

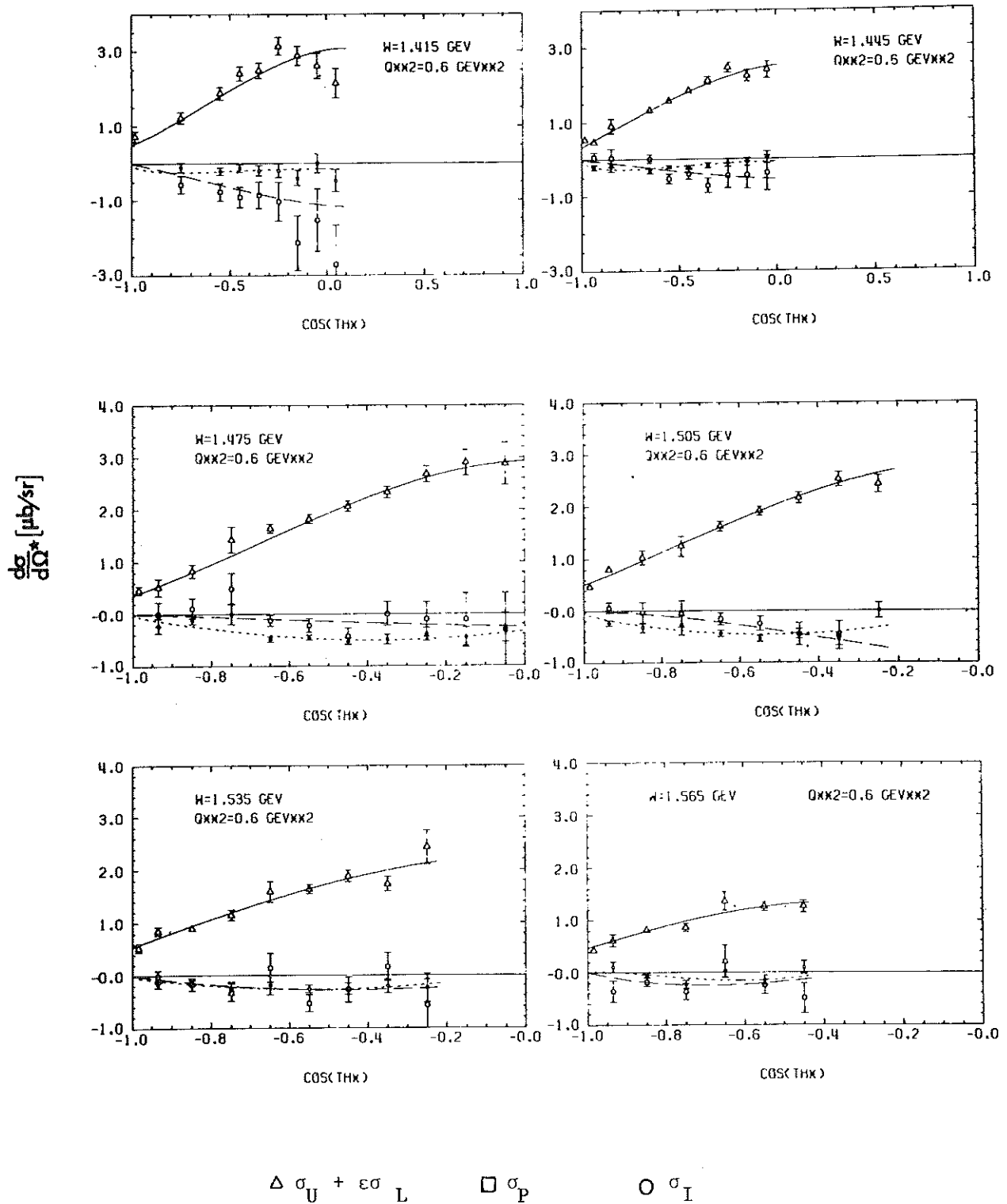


Fig. 5

$\gamma p \rightarrow \pi^0 p$

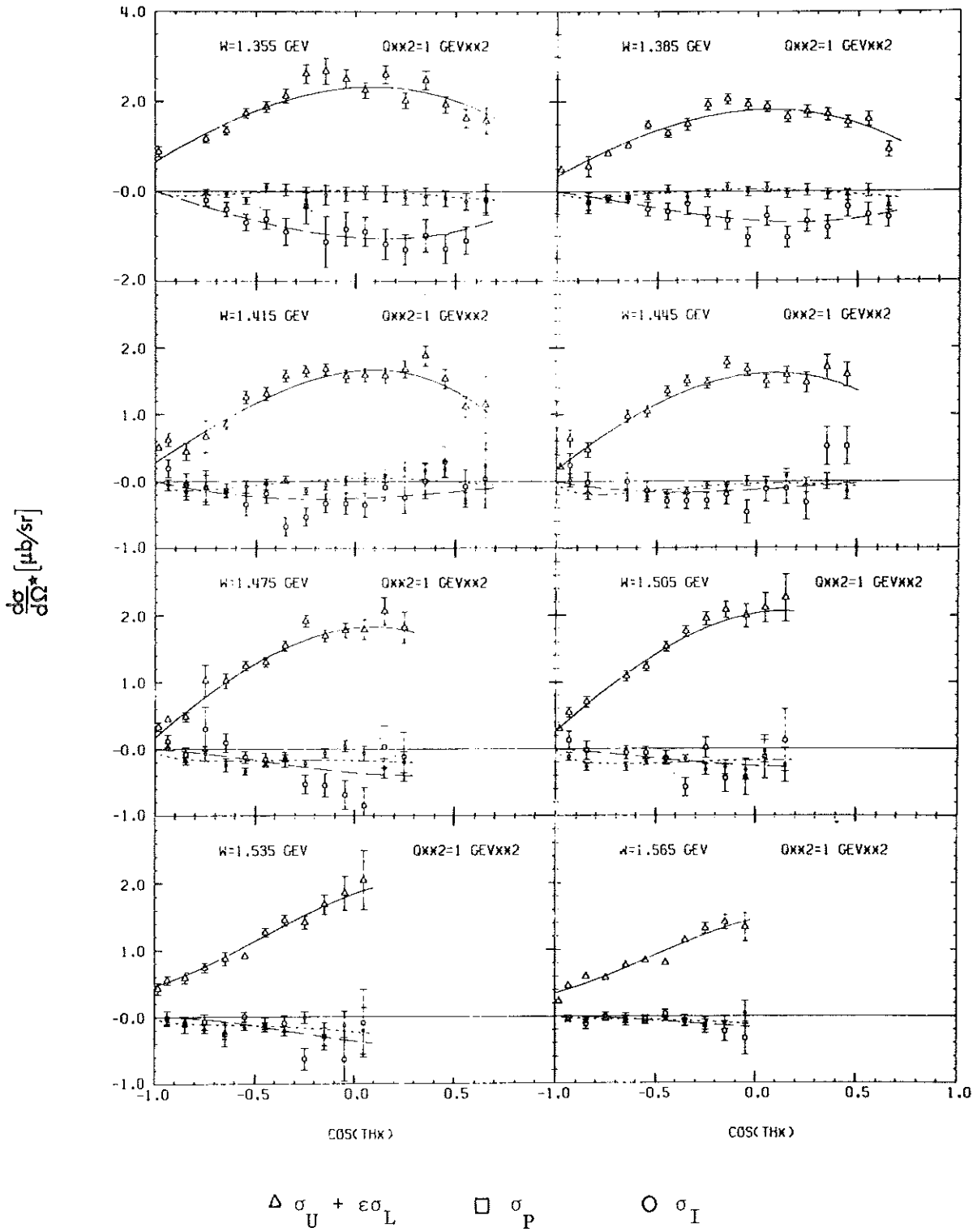
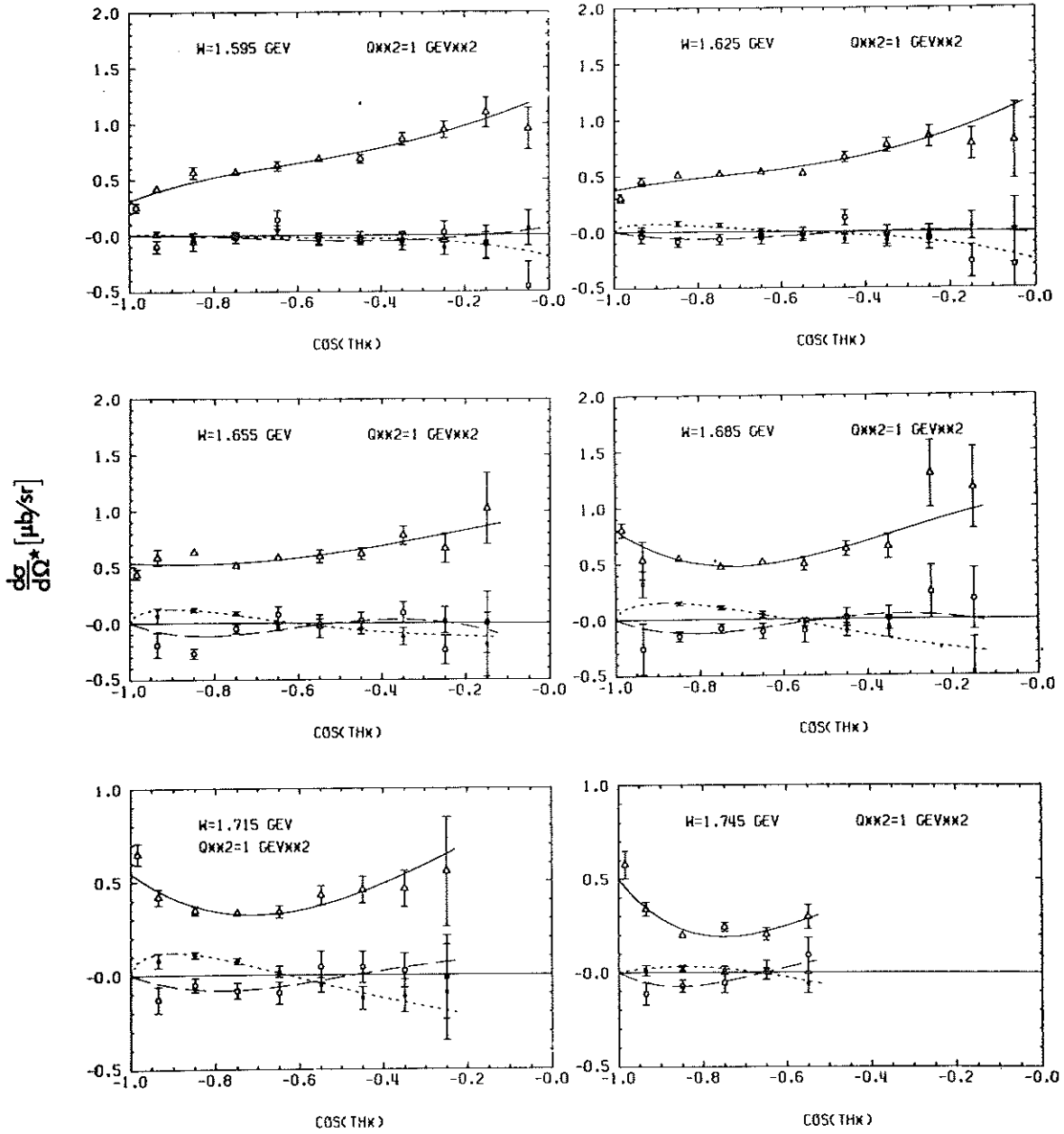


Fig. 6a

$\gamma_V p \rightarrow \pi^0 p$



$\Delta \sigma_U + \epsilon \sigma_L$ $\square \sigma_P$ $\circ \sigma_I$

Fig. 6b

$\gamma p \rightarrow \pi^0 p$

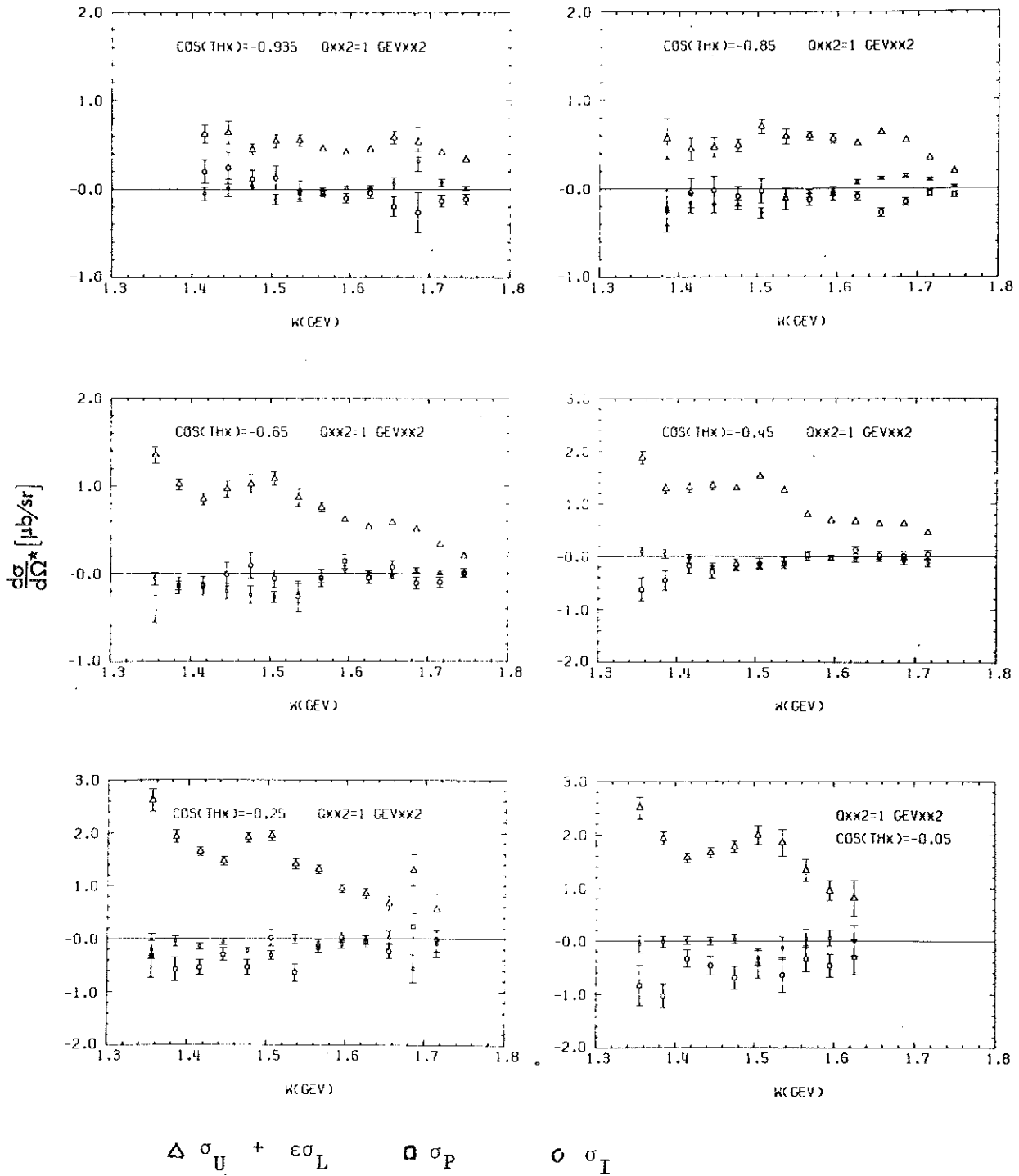
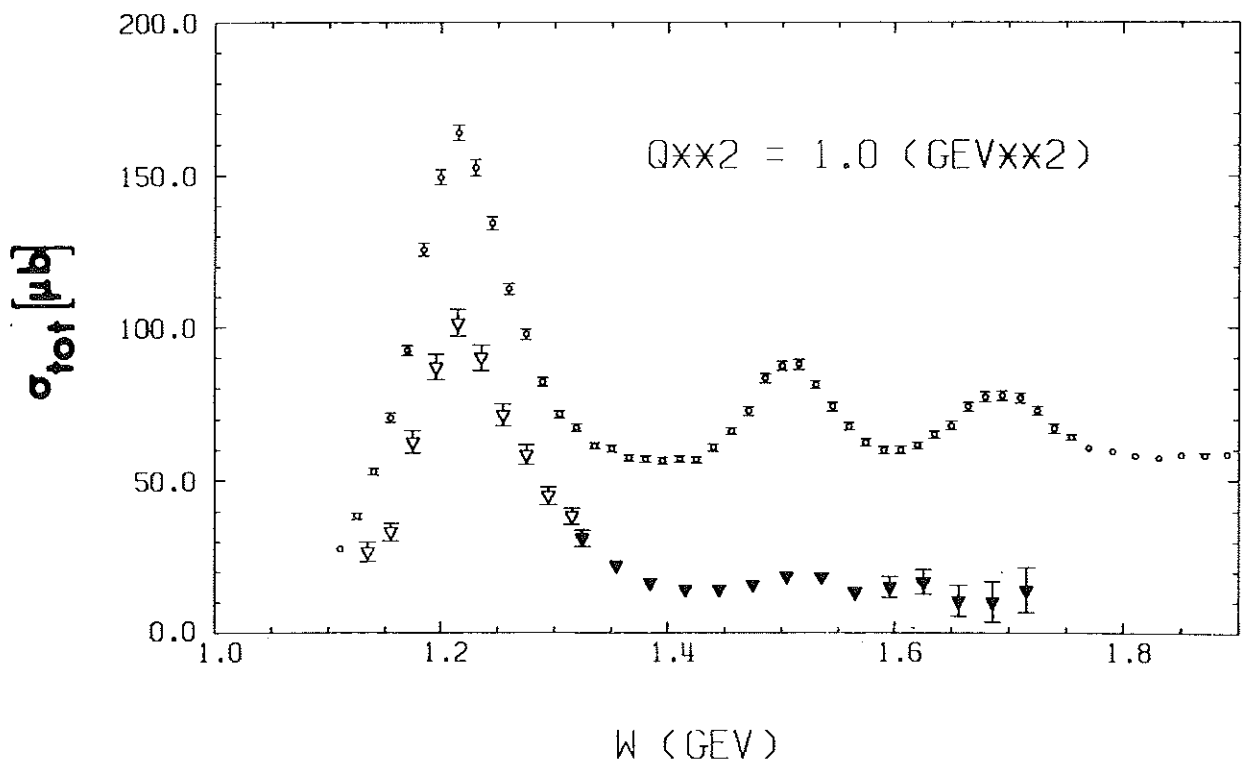
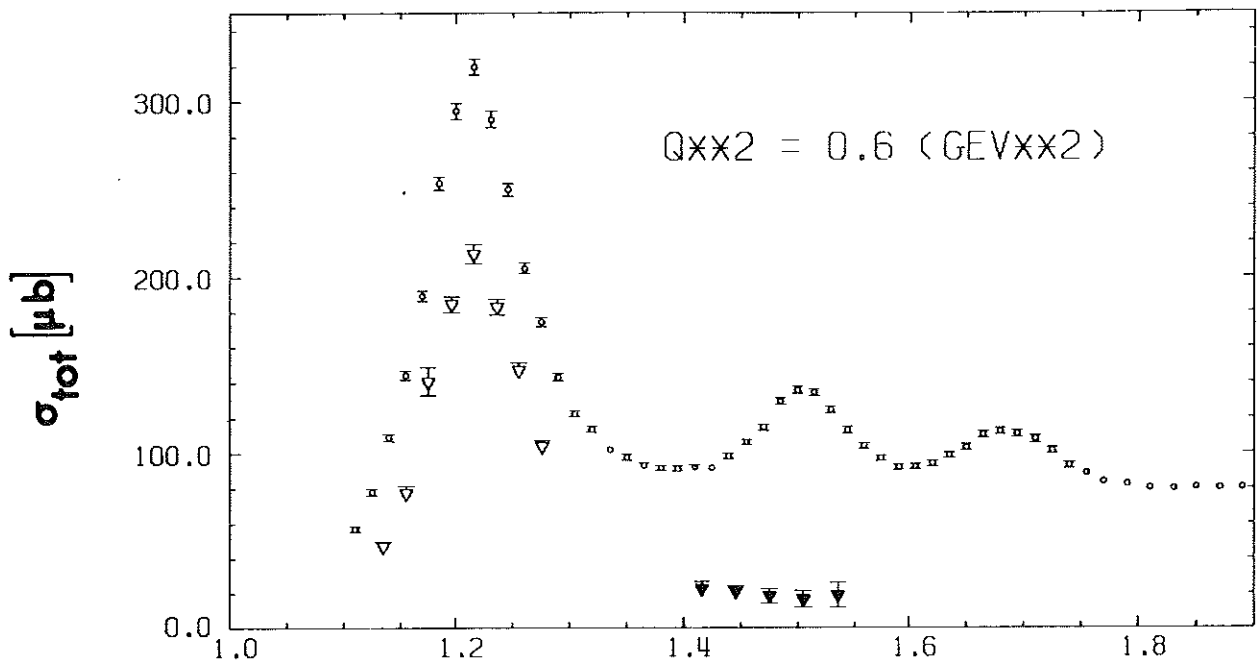


Fig. 7



$\nabla, \blacktriangledown \quad \gamma_{\nu} P \rightarrow \pi^0 P$

$\circ \quad \gamma_{\nu} P \rightarrow X$

Fig. 8